

## Direct Measurement of Spin-Dependent Conduction-Electron Mean Free Paths in Ferromagnetic Metals

Bruce A. Gurney, Virgil S. Speriosu, Jean-Pierre Nozieres, Harry Lefakis, Dennis R. Wilhoit, and Omar U. Need

IBM Research Division, Almaden Research Center, 650 Harry Road, San Jose, California 95120-6099  
(Received 13 April 1993)

Using a new giant magnetoresistance structure we measure the spin-up mean free paths of ferromagnetic metals. At room temperature we find for Co  $\lambda^+ = 55 \pm 4 \text{ \AA}$ , for Fe  $\lambda^+ = 15 \pm 2 \text{ \AA}$ , and for Ni<sub>80</sub>Fe<sub>20</sub> alloy  $\lambda^+ = 46 \pm 3 \text{ \AA}$ . Combining these results with the Mott picture of transport we deduce the spin-down mean free paths, and find for Co  $\lambda^- \lesssim 6 \text{ \AA}$ , for Fe  $\lambda^- = 21 \pm 5 \text{ \AA}$ , and for Ni<sub>80</sub>Fe<sub>20</sub>  $\lambda^- \lesssim 6 \text{ \AA}$ .

PACS numbers: 72.15.Lh, 75.50.Rr, 75.70.Cn

We describe a powerful method to determine the spin-up and spin-down conduction-electron mean free paths in ferromagnetic metals, using a new giant magnetoresistance (GMR) structure. Since Drude [1], models based on electron motion in metals have been successful predictors of the transport properties of elements and alloys. All such models are based on the mean free path (or, equivalently, relaxation time) between collision events, which could be determined in nonferromagnetic metals by measuring the resistance while changing the thickness in thin films as described by Fuchs [2] and Sondheimer [3]. With the advent of band theory, Mott [4,5] proposed that in transition metals the scattering from *s* to *d* bands dominates transport, and that because of the spin-split *d* states in ferromagnetic metals this scattering would lead to different mean free paths for the majority (spin-up) and minority (spin-down) carriers. Fert, Campbell, and others [6] were able to infer spin-dependent resistivities from transport in dilute binary and ternary ferromagnetic alloys, but their technique is unable to measure directly the mean free paths, and differing results were often obtained for the same system [7,8]. Our novel layered thin film structure acts as a spin-polarized conduction-electron source, enabling independent determination of majority and minority carrier mean free paths of ferromagnetic metals, including pure elements and concentrated alloys. Compared to recent modeling of GMR results that use spin-dependent mean free paths as fitting parameters [9–12] the present approach is much more direct. Recent GMR measurements perpendicular to the film plane [13] offer insight into mean free paths, but spin accumulation influences the results [14]. Our method is applicable from low temperatures to well above room temperature, offering great flexibility in probing magnon, phonon, and residual (defect) scattering in ferromagnetic metals.

We deduce the behavior of carriers from a new class of spin valve [15–18] structures (backed spin valves), shown schematically in Fig. 1(a). Previous spin valves consisted of two ferromagnetic conducting layers (*P* and *F*) separated by a nonmagnetic conducting spacer layer; by exchange anisotropy from an antiferromagnet the magnetization  $M_P$  of *P* (the pinned layer) was maintained as a

single domain whose direction was fixed in the small fields required to change the direction of the magnetization  $M_F$  of *F* (the free layer). Magnetoresistance was observed by applying a magnetic field sufficient to change the direction of  $M_F$  with respect to  $M_P$ . In the backed spin valve the free layer is replaced by two layers: Nearest the spacer is a thin ferromagnetic layer (filter layer), and behind is a conducting nonmagnetic or magnetic (i.e., back) layer whose properties are to be probed. We note that a different sandwich structure has recently been used to study spin accumulation in Au films [19].

Magnetic and magnetotransport measurements were made at room temperature (RT) on backed spin valves that were deposited [15] by magnetron sputtering. Results for the change in film conductance between parallel

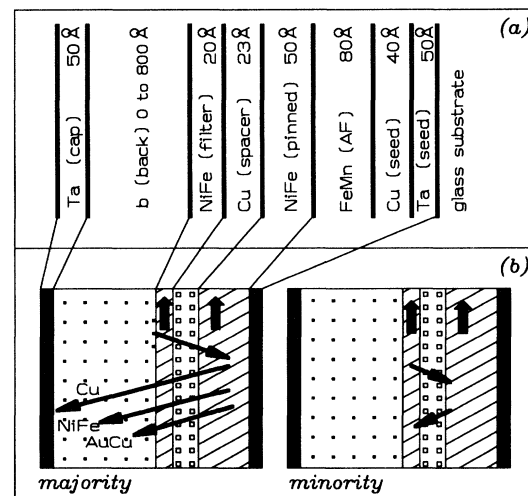


FIG. 1. (a) Layers in the new spin valve structure. (b) Schematic showing representative trajectories for electrons emanating from the ferromagnetic layers when the magnetizations are parallel, illustrating how back materials with differing majority carrier mean free paths lead to differing majority penetration depths, whereas for minority carriers the short penetration depth in Ni<sub>80</sub>Fe<sub>20</sub> assures they will be scattered before reaching the back layer.

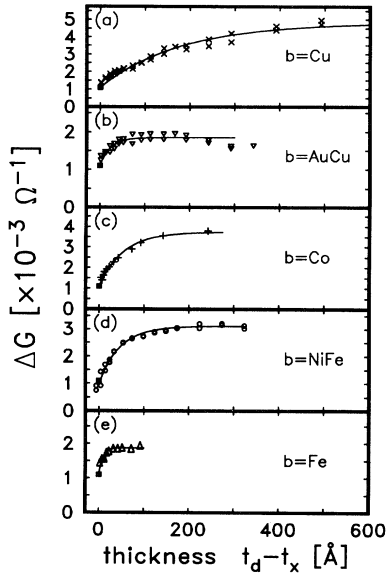


FIG. 2. Change in film conductance at room temperature between parallel and antiparallel magnetization states,  $\Delta G$ , vs the thicknesses of pure back layer  $t_d - t_x$ , where  $t_d$  is the deposited thickness and  $t_x$  is that of the intermixed interface; also shown is a fit by Eq. (1b) to obtain  $d_{\Delta G} = \lambda^+/\beta$ . Squares show the finite  $\Delta G$  from the filter layer alone.

and antiparallel magnetizations,  $\Delta G$  ( $\cong \Delta R/R^2$  where  $R$  is the sheet resistance), for glass/(50 Å)Ta/(40 Å)Cu/(80 Å)Fe<sub>50</sub>Mn<sub>50</sub>/(50 Å)Ni<sub>80</sub>Fe<sub>20</sub>/(23 Å)Cu/(20 Å)Ni<sub>80</sub>Fe<sub>20</sub>/( $t$  Å) $b$ /(50 Å)Ta structures, where  $b = \text{Cu, Ni}_{80}\text{Fe}_{20}, \text{Au}_{50}\text{Cu}_{50}, \text{Co, and Fe}$ , are shown in Fig. 2. The (50 Å)Ta/(40 Å)Cu seed layer provides a template to properly grow the Fe<sub>50</sub>Mn<sub>50</sub> for substantial exchange bias, and results in a small amount of current shunting but does not affect [20]  $\Delta G$ ; the other Ta layer is a protective cap. When grown in this order the layer  $b$  is deposited after the pinned, spacer, and filter layers; thus the properties of these layers remain independent of the thickness and choice of the  $b$  layer. We display  $\Delta G$  because we have shown, formally and by experiment [20], this to be the macroscopic quantity most directly related to the microscopic scattering leading to GMR for transport measured parallel to the layers. Note in Fig. 2 that there is an *increase* in magnetoconductance beyond that of Ni<sub>80</sub>Fe<sub>20</sub> when replacing most of the Ni<sub>80</sub>Fe<sub>20</sub> with a *nonmagnetic* metal (Cu), at first a surprising result. In the following discussion we show that this is a natural consequence of

how this structure probes the majority carrier mean free path in the  $b$  layer material.

To illustrate how our structure works Fig. 1(b) schematically shows representative electron trajectories when  $M_F$  and  $M_P$  are parallel for  $b = \text{Cu, Ni}_{80}\text{Fe}_{20}$ , and  $\text{Au}_{50}\text{Cu}_{50}$ . Shown are both the majority and minority carriers (with respect to the pinned layer) that originate in  $P$ . These are the carriers moving toward  $F$  that are able to be scattered differently when  $M_F$  is reversed, and that therefore lead to GMR. Those electrons contributing to GMR that are moving in the opposite direction, from  $F$  toward  $P$ , travel on average the same distance, so for simplicity we discuss only those starting from  $P$ . Irrespective of whether interface or bulk spin-dependent scattering is operative, for majority carriers  $F$  is transmitting, while for minority carriers penetration into  $F$  before scattering is  $\approx 4$  Å [21], as determined by the moving test layer method of Parkin [22]. Notice that for minority electrons emanating from  $P$  into the spacer, the short minority carrier penetration depth means that their number crossing the spacer and the distance they travel before their next scattering event is much smaller than for the majority carriers. Viewed in this way, the  $P$ , spacer, and  $F$  layers form a spin-polarized conduction-electron source [15,16] which we use to probe the scattering properties of the layer  $b$ . In particular, since minority carriers are scattered soon after entering  $F$ , but majority carriers pass generally unscattered into the layer  $b$ , the different magnetotransport obtained for different  $b$  strongly reflects the different majority carrier conductivity for material  $b$ .

Expanding on this qualitative picture we have modeled our results by applying a classical solution of the Boltzmann transport equation to our layered geometry that considers each layer to have a single majority and minority carrier mean free path. The current passing through each point in the structure is determined from the direction weighted integral over the carriers coming from the rest of the structure less the number scattered on the way (with probability  $e^{-l/\lambda_q^s}$  per unit length and  $\lambda_q^s$  the mean free path in layer  $q$  for spin  $s$ ). Our model is similar to that used by Diény [23] to describe less complicated spin valves. This picture is phenomenological in the sense that it does not calculate transport from the rich texture of behavior arising from each of the individual electronic bands, but describes the expected behavior in terms of the transport averaged over the Fermi surface in each layer; it is just these average properties that are probed by our structure. For the spin valve structure described here the change in conductance given by our model is

$$\Delta G \cong \Delta G_f + \Delta g_0 [\lambda_b^+ e^{-\beta t_f/\lambda_f^+} \{1 - e^{-\beta[(t_d - t_x)/\lambda^+]\}\} - \lambda_b^- e^{-\beta t_f/\lambda_f^-} \{1 - e^{-\beta[(t_d - t_x)/\lambda^-]\}\}] \quad (1a)$$

$$\approx \Delta G_f + \Delta G_b [1 - e^{-\beta[(t_d - t_x)/\lambda^+]\}] \quad (\lambda_f^- \ll \beta t_f), \quad (1b)$$

where  $\Delta G_f$  is the contribution from the filter part of  $F$  alone ( $1.1 \times 10^{-3} \Omega^{-1}$ ),  $\Delta g_0$  depends on the thicknesses and materials used in the  $P$ , spacer, and  $F$  layers (held the same throughout this experiment),  $t_f, \lambda_f^+, \lambda_f^-$  are the filter layer

thickness, majority, and minority carrier mean free paths, respectively, while  $\lambda^+$  and  $\lambda^-$  are the  $b$  layer mean free paths. The thickness of pure  $b$  layer present is the thickness of the deposited  $b$  layer ( $t_d$ ), less the thickness of the intermixed, high resistivity, regions ( $t_x$ ) formed at the  $b$  layer interfaces. The thicknesses of the intermixed regions have been measured [24–26] and the Cu/Ni<sub>80</sub>Fe<sub>20</sub> and Au<sub>50</sub>Cu<sub>50</sub>/Ni<sub>80</sub>Fe<sub>20</sub> interfaces are found to be 2 Å half width at half maximum. The intermixing of Ni<sub>80</sub>Fe<sub>20</sub>/Ta leads to a 6 Å layer with no moment at RT and high resistivity; we expect that  $t_x$  for Au<sub>50</sub>Cu<sub>50</sub>/Ta and Cu/Ta interfaces is also 6 Å. It is the key feature of our structure that when  $t_f \gg \lambda_f^-$  and  $t_f < \lambda_f^+$ , as is the case with a 20 Å Ni<sub>80</sub>Fe<sub>20</sub> filter layer, then the contribution to  $\Delta G$  in Eq. (1a) from the minority carriers in layer  $b$  is negligible, and Eq. (1b) results, where  $\Delta G_b = \Delta g_0 \lambda^+ e^{(-\beta t_f / \lambda_f^+)}$ . The exponentials of Eq. (1) are leading terms in asymptotic series solutions to the Boltzmann's equation;  $\beta$  results from the three-dimensional angle average of arriving carriers, and is of order unity [27]. Note that we measure the characteristic length scale of the rise of  $\Delta G$  with  $b$  layer thickness  $d_{\Delta G} = \lambda^+ / \beta$ . For  $b = \text{Cu}$  we obtain  $d_{\Delta G} = 192 \pm 22$  Å, which is nearly  $\lambda = 226 \pm 10$  Å obtained from the measured resistivity and the free electron model. Similarly, for  $b = \text{Au}_{50}\text{Cu}_{50}$  we find  $d_{\Delta G} = 22 \pm 4$  Å, compared to  $\lambda = 20 \pm 1$  Å derived from the Au<sub>50</sub>Cu<sub>50</sub> resistivity. This demonstrates that this spin valve structure measures the majority carrier mean free path in the layer  $b$  with  $\beta \approx 1$ . In the same way we are able to fit our results (Fig. 2) for ferromagnetic metals to obtain  $\lambda^+$  for Ni<sub>80</sub>Fe<sub>20</sub> ( $\lambda^+ = 46 \pm 3$  Å), Co ( $\lambda^+ = 55 \pm 4$  Å), and Fe ( $\lambda^+ = 15 \pm 2$  Å).

To determine the minority carrier mean free path in a ferromagnetic metal we could use our novel structure with a filter layer that was transmitting to minority carriers but which scattered majority carriers shortly after entering the filter, but such a material has not been firmly established. We choose instead to deduce  $\lambda^-$  using the contrast in GMR behavior between two  $b$  layers with comparable resistivity but where one layer is a ferromagnet (labeled  $M$ ) and the other is a nonferromagnet ( $N$ ). We illustrate the method with  $M = \text{Ni}_{80}\text{Fe}_{20}$  and  $N = \text{Au}_{50}\text{Cu}_{50}$  ( $1/\sigma = \rho \approx 23 \mu\Omega \text{ cm}$  for both alloys when deposited in our sputtering apparatus). All materials we have chosen for  $b$  have conduction bands that are free-electron-like. This is well known for Cu and Au, and is easily seen for their alloy. Although possessing more complicated band structures [28], transport in Ni, Fe, and Co is also dominated by free-electron-like behavior, derived mostly from the  $s$ - $p$  bands in some pictures [5], and from the  $d$  bands in others [29]; so a free electron picture of their transport is also a good estimate of their behavior. We connect the macroscopic conductances to microscopic scattering through the Boltzmann transport equation. In the relaxation time approximation the conductivity of a material is the sum over partially filled

bands  $x$  and both spins  $s$  of  $\sigma_{x,s} = n_{x,s} e^2 \tau_{x,s} / m_{x,s}^*$ , where  $n$  is the filling of the band,  $\tau_{x,s}$  is the relaxation time, and  $m_{x,s}^*$  is the effective mass. For the free-electron-like bands that dominate transport in these materials we can take  $\tau_{x,s} \approx \lambda_{x,s} / v_F$  where  $v_F = \hbar k_F / m_e$  is the Fermi velocity,  $m_{x,s}^* \approx m_e$ , and  $n$  from the Fermi level (any deviations can be included in a factor  $\eta_s = m_s^* / m_e$ ). Then the conductivity is simply  $\sigma_s \approx \eta_s (m_e e^2 / 3\pi^2 \hbar^3) E_F \lambda_s$ , where  $E_F$  is the Fermi energy. From this result and the conductivity we obtain  $\lambda^-$  in the ferromagnet  $M$  from  $\lambda^+$  in  $M$  (obtained from  $d_{\Delta G}$  when  $b = M$ ) and from  $\lambda$  in the nonferromagnet (obtained when  $b = N$ )

$$\lambda_M^- = 2 \left( \frac{\eta_N}{\eta_M^-} \right) \left( \frac{E_{FN}}{E_{FM}} \right) \left( \frac{\rho_N}{\rho_M} \right) \lambda_N - \left( \frac{\eta_M^+}{\eta_M^-} \right) \lambda_M^+. \quad (2)$$

Using this result, published Fermi energies [28], and the resistivities of our films ( $\rho_{\text{Ni}_{80}\text{Fe}_{20}} = 24$ ,  $\rho_{\text{Cu}} = 2.8$ ,  $\rho_{\text{Au}_{50}\text{Cu}_{50}} = 22$ ,  $\rho_{\text{Co}} = 14.8$ ,  $\rho_{\text{Fe}} = 20 \mu\Omega \text{ cm}$ ), we obtain  $\lambda^-$  for Ni<sub>80</sub>Fe<sub>20</sub> ( $\lambda^- \lesssim 6$  Å), Co ( $\lambda^- \lesssim 10$  Å), and Fe ( $\lambda^- = 21 \pm 5$  Å), if we set  $\eta_N = \eta_M^+ = \eta_M^- = 1$ . Taking  $\eta^+ = 1$  in the case of Ni<sub>80</sub>Fe<sub>20</sub> and Co is justified since mostly  $s$ - $p$  bands cross the Fermi surface; however, due to  $d$  band crossings  $\eta^- = 1$  is an approximation. But since the values obtained for  $\lambda^-$  are so small the influence of this deviation will be minimal on the overall result. Thus we have demonstrated an order of magnitude difference between  $\lambda^+$  and  $\lambda^-$  in these metals. We note that the  $\lambda^-$  for Ni<sub>80</sub>Fe<sub>20</sub> we obtain is the same as the distance that minority carriers emanating from one ferromagnetic layer penetrate into the other ferromagnetic layer before scattering [21,22] in Ni<sub>80</sub>Fe<sub>20</sub>/Cu spin valves. Thus no special interfacial spin-dependent scattering need be invoked to describe the GMR in this system, as was less directly shown by Dieny [10]. In Fe both spins have substantial  $d$  character at the Fermi surface [29], and the exact value of  $\lambda^-$  awaits detailed calculation of  $\eta_s$ , but our results indicate that  $\lambda^- \approx \lambda^+ \approx 15$  Å. This suggests that in Fe based multilayers interfacial spin-dependent scattering is necessary to obtain substantial GMR, as was originally suggested [30] and later confirmed [31].

Our results are consistent with the two current picture of transport in ferromagnetic transition metals and their band structure. The substantial difference in the spin-split density of states (DOS) at the Fermi level of Co [28] leads to an order of magnitude difference in  $\lambda^+$  and  $\lambda^-$ . In Ni<sub>80</sub>Fe<sub>20</sub>  $\lambda^+ \gg \lambda^-$ , consistent with the large spin-split DOS in the similar metal Ni [28], and in agreement with earlier work [6] where a ratio of spin-up to spin-down resistivities of about 10 was inferred in bulk dilute alloys, and also in recent layer Korringa-Kohn-Rostoker calculations [32]. For Fe the DOS at the Fermi level for spin-up is somewhat greater than for spin-down electrons [28], consistent with the  $\lambda^- \gtrsim \lambda^+$  we obtain. In our analysis we have assumed  $\eta^+ = \eta^- = 1$  and  $k_F^+ = k_F^-$

as did Mott [4,5], and obtained results consistent with what that picture predicts. In an alternative picture [29] transport is dominated by  $d$  band carriers with  $\eta^+ > \eta^-$  and  $k_F^+ > k_F^-$ ; adoption of this model would result in different values of  $\lambda^-$ , although our central result that  $\lambda^+ \gg \lambda^-$  for  $\text{Ni}_{80}\text{Fe}_{20}$  and Co remains unchanged. We expect the use of backed spin valves with appropriate filter layers to measure both  $\lambda^+$  and  $\lambda^-$  directly will distinguish between these two pictures. Also, backed spin valves probing alloy  $b$  layers where the Fermi level is swept through the transition metal bands can be used to distinguish between these two pictures by correlating the asymmetry  $\lambda^+/\lambda^-$  with different  $d$  and  $s$ - $p$  band features. In summary, we have developed a method to determine the spin-dependent mean free paths of conduction electrons in ferromagnetic transition metals. We find that  $\text{Ni}_{80}\text{Fe}_{20}$  and Co show a substantial difference between  $\lambda^+$  and  $\lambda^-$ , whereas in Fe they are nearly equal.

- 
- [1] P. Drude, *Ann. Phys. (Leipzig)* **3**, 369 (1900).  
 [2] K. Fuchs, *Proc. Cambridge Philos. Soc.* **34**, 100 (1938).  
 [3] H. Sondheimer, *Adv. Phys.* **1**, 1 (1952).  
 [4] N. Mott, *Proc. R. Soc.* **156**, 368 (1936).  
 [5] N. Mott, *Adv. Phys.* **13**, 325 (1964).  
 [6] I. Campbell and A. Fert, *Ferromagn. Mater.* **3**, 747 (1982).  
 [7] T. Farrell and D. Greig, *J. Phys. C* **1**, 1359 (1968).  
 [8] J. Dorleijn and A. Miedema, *J. Phys. F* **5**, 487 (1975).  
 [9] A. Barthelemy and A. Fert, *Phys. Rev. B* **43**, 13 124 (1991).  
 [10] B. Dieny, *Europhys. Lett.* **17**, 261 (1992).  
 [11] P. Levy, S. Zhang, and A. Fert, *Phys. Rev. Lett.* **65**, 1643 (1990).  
 [12] B. Johnson and R. Camley, *Phys. Rev. B* **44**, 9997 (1991).  
 [13] W. Pratt, Jr., S. Lee, J. Slaughter, R. Lolee, P. Schroeder, and J. Bass, *Phys. Rev. Lett.* **66**, 3060 (1991).  
 [14] T. Valet and A. Fert, *J. Magn. Magn. Mater.* **121**, 378 (1993).  
 [15] B. Dieny, V. Speriosu, B. Gurney, S. Parkin, D. Wilhoit, K. Roche, S. Metin, D. Peterson, and S. Nadimi, *J. Magn. Magn. Mater.* **93**, 101 (1991).  
 [16] B. Dieny, V. Speriosu, S. Parkin, B. Gurney, D. Wilhoit, and D. Mauri, *Phys. Rev. B* **43**, 1297 (1991).  
 [17] B. Dieny, V. Speriosu, S. Metin, S. Parkin, B. Gurney, P. Baumgart, and D. Wilhoit, *J. Appl. Phys.* **69**, 4774 (1991).  
 [18] B. Dieny, P. Humbert, V. Speriosu, S. Metin, B. Gurney, P. Baumgart, and H. Lefakis, *Phys. Rev. B* **45**, 806 (1992).  
 [19] M. Johnson, *Phys. Rev. Lett.* **70**, 2142 (1993).  
 [20] B. Dieny, J. Nozieres, V. Speriosu, B. Gurney, and D. Wilhoit, *Appl. Phys. Lett.* **61**, 2111 (1992).  
 [21] B. Gurney, J. Nozieres, V. Speriosu, H. Lefakis, D. Wilhoit, and O. Need, in Proceedings of the EMRS Symposium on Magnetic Thin Films, Lyon, France, 7-11 September 1992 (unpublished); (to be published).  
 [22] S. Parkin, in Proceedings of the 13th International Conference on Magnetic Films and Surfaces, Glasgow, Scotland, 26-30 August 1991 (unpublished).  
 [23] B. Dieny, *J. Phys. Condens. Matter* **4**, 1 (1992).  
 [24] V. Speriosu, J. Nozieres, B. Gurney, B. B. Dieny, T. Huang, and H. Lefakis, *Phys. Rev. B* **47**, 11 579 (1993).  
 [25] T. Huang, J. Nozieres, V. Speriosu, B. Gurney, and H. Lefakis, *Appl. Phys. Lett.* **62**, 1478 (1993).  
 [26] J. Nozieres, V. Speriosu, B. Gurney, B. Dieny, T. Huang, and H. Lefakis, *J. Magn. Magn. Mater.* **121**, 386 (1993).  
 [27] B. Gurney, V. Speriosu, and D. Wilhoit (to be published).  
 [28] D. Papaconstantopoulos, *Handbook of the Band Structure of Elemental Solids* (Plenum, New York, 1986).  
 [29] M. Stearns, *J. Magn. Magn. Mater.* **5**, 167 (1977).  
 [30] M. Baibich, J. J. M. Broto, A. Fert, N. Van Dau, F. Petroff, P. Eitienne, G. Creuzet, A. Friedrich, and J. Chazelas, *Phys. Rev. Lett.* **61**, 2472 (1988).  
 [31] P. Baumgart, B. Gurney, D. Wilhoit, T. Nguyen, B. Dieny, and V. Speriosu, *J. Appl. Phys.* **69**, 4792 (1991).  
 [32] W. Butler, J. MacLaren, and X. Zhang, *Mater. Res. Soc. Symp. Proc.* **313**, 59 (1993).